Available online at www.sciencedirect.com
ScienceDirect
Journal of Solid State Chemistry 180 (2007) 1750–1758
JOURNAL OF SOLID STATE CHEMISTRY
www.elsevier.com/locate/jssc

Three new tellurite halides with unusual Te^{4+} coordinations and iron honeycomb lattice variants

Richard Becker*, Mats Johnsson

Inorganic Chemistry, Stockholm University, SE-106 91 Stockholm, Sweden

Received 25 January 2007; received in revised form 5 March 2007; accepted 12 March 2007
Available online 19 March 2007

Abstract

The crystal structure of three new iron and copper-iron tellurite halides are presented; (**I**) $Cu_3Fe_8Te_{12}O_{32}Cl_{10}$ that crystallizes in the orthorhombic space group *Pmmn*, (**II**) $Fe_8Te_{12}O_{32}Cl_3Br_3$ that crystallizes in the monoclinic space group $P2_1/c$, and (**III**) $Fe_5(TeO_3)_6Cl_2$ that crystallizes in the triclinic space group *P*-1. The crystal structures were solved from single crystal X-ray diffraction data. All three compounds have layered crystal structures where the Fe atoms form variants of the honeycomb lattice. Highly unusual Te^{4+} coordination polyhedra are exemplified: $[TeO_{3+1}E]$, $[TeO_3XE]$, $[TeO_{3+1}XE]$, and $[TeO_3X_2E]$ (X = halide ion, E = the lone–pair valence electrons). The crystal structures contain large non-bonding volumes occupied by the stereochemically active lone–pair electrons on Te^{4+}.

Keywords: Crystal structure determination; Iron; Oxo-halide; Lone–pair elements; Tellurites

1. Introduction

During the past few years, a synthesis strategy has been developed for finding new inorganic compounds showing a low-dimensional arrangement of transition metal cations. The concept is based on forming oxohalides comprising p-element cations having stereochemically active lone–pairs. Te^{4+} is the lone–pair cation that mainly has been utilized in these studies, but also Se^{4+} and Sb^{3+} have been exploited to some extent. The lone–pair electrons, E, occupy a non-bonding orbital that is stereochemically active and can therefore be regarded as an additional ligand completing the coordination polyhedron. In addition to the lone–pair cations, halide ions having low coordination numbers also help to open up the crystal structures. The synthesis concept has proved to be successful and several new structurally low-dimensional compounds and even quantum spin compounds have been described [1–7]. A majority of the work conducted so far has been focused on using weak and moderately weak Lewis acids as transition metal cations, e.g. Cu^{2+} and Co^{2+}, allowing comparatively strong Te–O bonds to form. The high Lewis acidity of Fe^{3+} will on the other hand allow for comparatively strong Fe–O bonds to form, and this may force Te^{4+} to accept halides as ligand. This is the case in, e.g. $FeTe_2O_5X$ (X = Cl, Br) in which Te^{4+} has a highly unusual $[TeO_2X]$ coordination [8].

This work presents the crystal structure of three new tellurite halide compounds with Fe present as transition metal; (**I**) $Cu_3Fe_8Te_{12}O_{32}Cl_{10}$, (**II**) $Fe_8Te_{12}O_{32}Cl_3Br_3$, and (**III**) $Fe_5(TeO_3)_6Cl_2$ (see Supplementary materials). The new compounds have in common that they are layered and show honeycomb or honeycomb like lattice arrangements of the Fe cations, as well as unusual Te^{4+} coordinations that in addition to oxygen also involve halides located at the verge of the primary coordination sphere.

2. Experimental

2.1. Synthesis

Three new compounds (**I**) $Cu_3Fe_8Te_{12}O_{32}Cl_{10}$, (**II**) $Fe_8Te_{12}O_{32}Cl_3Br_3$, and (**III**) $Fe_5(TeO_3)_6Cl_2$ were synthesized

*Corresponding author. Fax: +46 8 15 21 87.
E-mail addresses: richard@inorg.su.se (R. Becker), matsj@inorg.su.se (M. Johnsson).

0022-4596/$ - see front matter © 2007 Elsevier Inc. All rights reserved.
doi:10.1016/j.jssc.2007.03.013

via chemical reactions in evacuated (~1 Torr) and sealed silica tubes with Ø = 6 mm and $l \approx 60$ mm. TeO_2 (ABCR 99.9%), CuO (ABCR Ltd. 99 + %), $TeBr_4$ (ABCR GmbH & Co. KG 99.9%), Fe_2O_3 (ChemPur Feinchemikalien und Forschungsbedarf GmbH 99.999%), $FeCl_3$ (ABCR GmbH & Co. KG 99%) and $FeCl_2$ (Sigma Aldrich 98%) were used as starting materials.

I was synthesized from a mixture of TeO_2:CuO:$FeCl_2$ in the off-stoichiometric molar ratio 2:1:1 in a muffle furnace at 540 °C for 70 h. The synthesis involves a red-ox reaction were Cu^{2+} is reduced to Cu^{+} and were also part of the starting Fe^{2+} has oxidized to Fe^{3+}. **II** was synthesized from a mixture of TeO_2:$TeBr_4$:Fe_2O_3:$FeCl_3$ in the off-stoichiometric molar ratio 45:3:10:4 in a muffle furnace at 530 °C for 46 h. Attempts to synthesize either of the two end Cl and Br components has so far been unsuccessful. The sample was prepared in a glove-box with argon atmosphere. **III** was prepared from a mixture of TeO_2:-$TeCl_4$:Fe_2O_3:$FeCl_3$ in the off-stoichiometric molar ratio 45:3:10:4 in a muffle furnace at 500 °C for 46 h. All the synthesis experiments resulted in a mixture of black single crystals of the title compounds and yellow platelets of either $FeTe_2O_5Cl$ or $FeTe_2O_5Cl_{0.5}Br_{0.5}$ [8]. **I** and **II** were only found as a few crystals during the synthesis, while **III** was found as several crystals although always present together with $FeTe_2O_5Cl$. Red-ox reactions also took place during the synthesis of **II** and **III,** where part of the Fe^{3+} was reduced to Fe^{2+}, and then most likely also part of the Te^{4+} was oxidized to Te^{6+}. However, no compounds have been identified in the synthesis products containing Te^{6+}. All three compounds are stable in air.

The chemical composition of the synthesis products were confirmed with energy-dispersive spectrometry analysis (EDS, LINK AN10000), which uses elemental Co as internal standard, in a scanning electron microscope (SEM, JEOL 820).

2.2. Single crystal X-ray diffraction

The crystal structures for **I–III** were solved from single-crystal X-ray data collected on an Oxford Diffraction Xcalibur3 diffractometer equipped with a sapphire CCD detector with use of graphite-monochromatized Mo $K\alpha$ radiation, $\lambda = 0.71073$ Å. The intensities of the reflections were integrated using the software supplied by the manufacturer. Gaussian face indexing absorption correction was performed with the programs Crysalis CCD [9] and Crysalis RED [10]. The structures were solved by direct methods using the program SHELXS97 [11], and refined by full matrix least squares on F^2 using the program SHELXL97 [12]. Crystallographic data for **I–III** are reported in Table 1.

3. Results

Three new tellurite halide compounds; **(I)** $Cu_3Fe_8Te_{12}O_{32}Cl_{10}$, **(II)** $Fe_8Te_{12}O_{32}Cl_3Br_3$ and **(III)** $Fe_5(TeO_3)_6Cl_2$ are synthesized and their structures are determined. The two valence electrons of Te^{4+} occupies a stereochemically active non-bonding orbital and can therefore be regarded as an additional ligand completing the coordination polyhedra of Te^{4+}. These lone–pair electrons are denoted as *E* below.

All atoms are refined with anisotropic temperature parameters. Atomic coordinates for **I–III** are listed in Tables 2a–c. Selected bonding distances for **I–III** are listed in Tables 3a–c.

The operational definition of a bond according to Brown is used when discussing primary bonds [13]. This definition states that a bond exists between a cation and an anion if its experimental bond valence is larger that 4% of the cation valence, and this has been used strictly in the structural descriptions. The maximum primary bonding distances for Te^{4+} that thus have been defined and applied in this work are: Te–O = 2.66 Å, Te–Cl = 3.05 Å, and Te–Br = 3.23 Å. r_0 values are listed in Table 4. For comparison, the maximum bonding distance for iron–oxygen bonds are: Fe^{2+}–O = 2.63 Å and Fe^{3+}–O = 2.55 Å.

3.1. The crystal structure of $Cu_3Fe_8Te_{12}O_{32}Cl_{10}$ (I)

I crystallizes in the orthorhombic system, space group *Pmmn*. The structure is layered perpendicular to [1 0 0] with separate Cu–Cl units, see Fig. 1a. EDS analyses on the same crystal as used for the collection of single crystal X-ray diffraction data determined the amount of the heavy atoms to be 8.6 ± 0.3 at% Cu, 23.8 ± 0.3 at% Fe, 36.4 ± 0.5 at% Te and 31.2 ± 0.5 at% Cl which is in good agreement with the results from the structural refinement (the errors have been estimated from ten different analysis on the same crystal).

The two crystallographically different Te^{4+} both coordinate to three oxygen atoms in a one-sided pyramidal coordination due to the presence of the stereochemically active lone–pair electrons. The Te–O distances are in the range 1.832(6)–1.949(8) Å, and the next oxygen is ~2.9 Å away from Te and thus clearly too far away to be considered as bonded. Each Te atom has a Cl rather close: the Te(1)–Cl(1) distance is 2.950(4) Å and the Te(2)–Cl(3) distance is 3.007(2) Å, and they are then just inside the primary bonding sphere according to Brown. The coordination polyhedra around the two Te can thus be considered to be [TeO_3ClE] trigonal bipyramids.

There is one crystallographically unique Fe atom that coordinates six oxygens in an octahedral fashion with Fe–O distances in the range 1.927(7)–2.176(6) Å. Each [FeO_6] octahedron is connected by edge sharing to two others and by corner sharing to one more to form layers. Each [FeO_6] octahedron also shares corners with six [TeO_3ClE] trigonal bipyramids. The Fe atoms are arranged into a honeycomb lattice, see Fig. 1b.

In between the Fe–Te–O layers there are Cu–Cl chains that are made up of half-occupied Cu^{+} and fully occupied Cl atoms, see Fig. 2a. An electron density map for the three

Table 1
Crystallographic data for I–III

Chemical formula	$Cu_3Fe_8Te_{12}O_{32}Cl_{10}$	$Fe_8Te_{12}O_{32}Cl_3Br_3$	$Fe_5(TeO_3)_6Cl_2$
Formula weight	3035.12	2836.08	1403.75
Temperature	19(3) °C	19(3) °C	19(3) °C
Wavelength	0.71073 Å	0.71073 Å	0.71073 Å
Crystal system	Orthorhombic	Monoclinic	Triclinic
Space group	*Pmmn* (No. 59)	$P2_1/c$ (No. 14)	*P*-1 (No. 2)
Unit cell dimensions	$a = 20.697(7)$ Å	$a = 9.921(3)$ Å	$a = 4.901(6)$ Å
	$b = 9.996(4)$ Å	$b = 5.0109(5)$ Å	$b = 10.381(5)$Å
	$c = 4.994(2)$ Å	$c = 36.7749(10)$ Å	$c = 9.256(8)$ Å
			$\alpha = 105.61(6)^\circ$
		$\beta = 90.710(8)^\circ$	$\beta = 104.32(7)^\circ$
			$\gamma = 90.43(7)^\circ$
Volume (Å^3)	1033.1(6)	1828.0(6)	438.1(7)
Z	1	2	2
D_{calcd}	4.878 g cm^{-3}	5.152 g cm^{-3}	5.320 g cm^{-3}
Absorption corr.	Gaussian	Gaussian	Gaussian
μ	13.280 mm^{-1}	16.073 mm^{-1}	14.231 mm^{-1}
$F(000)$	1345	2488	620
Crystal colour	Black	Black	Black
Crystal habit	Plate	Needle	Needle
Crystal size (mm)	0.050 × 0.020 × 0.003	0.195 × 0.030 × 0.017	0.084 × 0.010 × 0.05
θ range for data collec.	3.93–26.43°	3.88–26.94°	4.08–25.94°
Index ranges	$-25 \leqslant h \leqslant 23$, $-12 \leqslant k \leqslant 12$, $-6 \leqslant l \leqslant 5$	$-12 \leqslant h \leqslant 12$, $-6 \leqslant k \leqslant 6$, $-46 \leqslant l \leqslant 46$	$-6 \leqslant h \leqslant 6$, $-12 \leqslant k \leqslant 12$, $-11 \leqslant l \leqslant 11$
Reflections collected	9711	16 815	1710
Independent reflections	1167 [R(int) = 0.0826]	3929 [R(int) = 0.0488]	1424 [R(int) = 0.0428]
Completeness to θ = max°	99.7%	98.2%	99.7%
Refinement method	Full-matrix least squares on F^2	Full-matrix least squares on F^2	Full-matrix least squares on F^2
Data/restraints/parameters	1167/0/93	3929/0/262	1710/0/142
Goodness-of-fit on F^2	1.018	0.998	1.503
Final R indices	$R1 = 0.0375$	$R1 = 0.0275$	$R1 = 0.0369$
[$I > 2\sigma$(I)]	w$R2 = 0.0834$	w$R2 = 0.0558$	w$R2 = 0.0452$
R indices	$R1 = 0.0592$	$R1 = 0.0437$	$R1 = 0.1387$
(all data)	w$R2 = 0.0907$	w$R2 = 0.0576$	w$R2 = 0.1411$
Largest diff. peak and hole (e Å^{-3})	1.911 and −1.533	1.062 and −1.620	1.082 and −2.984

copper sites is shown in Fig. 2b. Cu(2) and Cu(3) show rather regular [$CuCl_4$] tetrahedra, with Cu–Cl distances in the range 2.262(5)–2.449(6) Å. The [$Cu(2)Cl_4$] and the [$Cu(3)Cl_4$] tetrahedra have a common edge so that chains are formed along [0 0 1]. Cu(1) is located on the common edge between two tetrahedra resulting in that it has an almost linear Cl(2)–Cu(1)–Cl(2) coordination with an angle of 175.7(5)°. A linear coordination for Cu^+ is present in, e.g. $CuGaO_2$, $CuTh_2(PO_4)_3$, and $CsCu_3S_2$ [14–16]. The Cu(1)–Cl(2) distance is 2.037(5) Å, while the Cu(1)–Cu(2) and Cu(1)–Cu(3) 'distances' are around 1.3 Å. The half-occupancies of the three Cu^+ sites can be interpreted so that each of the sites are fully occupied every second time. This will result in Cu_2Cl_6 dimers separated by $CuCl_2$ units, see Fig. 2a. The coordination around Cu(1) can also be regarded as a highly distorted octahedral coordination with the two Cu(1)–Cl(2) distances as short as 2.038(4) Å and four very long Cu(1)–Cl(1) distances in the equatorial plane at 3.030(7) and 3.348(7) Å.

Each Cl(1) is weakly bonded to Te(1) as discussed above, and this long bond is the only connection between the Fe–Te–O layers and the Cu–Cl chains. Cl(3) is located along [0 0 1] between the Fe–Te–O layers, and they can also be regarded as linking the Fe–Te–O layers via four long Te(2)–Cl(3) distances at 3.007(2) Å, see Fig. 1a.

For the compound to gain charge neutrality we need to consider the possible oxidation states for the cations. The one-sided coordination around the tellurium atoms has been taken as a sign for that they both are Te^{4+}. The sum of the charges for Te, O, and Cl leaves a net charge of −26 which should be balanced by the eight Fe- and the three Cu atoms in the formula unit. The coordination of Cu as well as the bond valence sum (BVS) calculations suggests that Cu is present exclusively as Cu^+, which leaves a net charge of −23 to be filled by the eight Fe ions. This means an average charge on each Fe ion of +2.875, or a 7:1 ratio of Fe^{3+}:Fe^{2+}, and this is supported by BVS calculations, which yields a valence of 2.89 for the single Fe site, see Table 4. The black colour of the crystals can also be seen substantiating the mixed valence of Fe, as such compounds often are black [17–19].

The half-occupancies of the three Cu positions could be resolved if the *c*-axis doubles, and the number of atoms are doubled except for the Cu atoms that then become fully occupied on one site each. However, no evidence for such a cell doubling is observed in, e.g. the 1 *k l* layer, see Fig. 3.

Table 2
Atomic coordinates and equivalent isotropic displacement parameters for (a) $Cu_3Fe_8Te_{12}O_{32}Cl_{10}$, (b) $Fe_8Te_{12}O_{32}Cl_3Br_3$, and (c) $Fe_5(TeO_3)_6Cl_2$

Atom	Wyck.	Occ.	x	y	z	U_{eq} [a] (Å^2)
(a)						
Te(1)	4*f*		0.93422(4)	1/4	0.2939(2)	0.0131(3)
Te(2)	8*g*		0.85973(3)	−0.07455(6)	0.7488(1)	0.0162(2)
Fe(1)	8*g*		0.97707(7)	−0.0785(1)	0.2452(2)	0.0150(3)
Cu(1)	2*b*		3/4	1/4	0.290(2)	0.049(2)
Cu(2)	2*b*		3/4	1/4	0.050(1)	0.038(2)
Cu(3)	2*b*		3/4	1/4	0.578(1)	0.044(2)
Cl(1)	4*f*		0.8457(2)	1/4	0.8309(7)	0.0288(9)
Cl(2)	4*e*		3/4	0.4537(4)	0.3055(8)	0.050(1)
Cl(3)	2*a*		3/4	−1/4	0.929(1)	0.032(1)
O(1)	8*g*		0.9349(3)	0.0011(6)	0.574(1)	0.014(1)
O(2)	4*f*		0.9970(4)	1/4	0.585(2)	0.013(2)
O(3)	8*g*		0.9759(3)	0.1140(6)	0.1000(1)	0.013(1)
O(4)	8*g*		0.8934(3)	−0.1030(7)	0.083(1)	0.022(2)
O(5)	4*f*		0.8798(4)	−1/4	0.607(2)	0.018(2)
(b)						
Te(1)	4*e*		0.12181(4)	−0.33929(9)	−0.17128(1)	0.0084(1)
Te(2)	4*e*		−0.23716(4)	−0.85298(9)	−0.21018(1)	0.0093(1)
Te(3)	4*e*		−0.03646(4))	−0.30689(8)	−0.05908(1)	0.0094(1)
Te(4)	4*e*		0.60676(4)	−0.81314(8)	−0.09321(1)	0.0092(1)
Te(5)	4*e*		0.31615(5)	−0.38037(9)	−0.04358(1)	0.0110(1)
Te(6)	4*e*		0.42789(5)	−0.74713(9)	−0.21301(1)	0.0095(1)
Fe(1)	4*e*		−0.0602(1)	−0.8226(2)	−0.12627(3)	0.0092(2)
Fe(2)	4*e*		−0.2263(1)	−0.3267(2)	−0.14422(3)	0.0086(2)
Fe(3)	4*e*		0.2168(1)	−0.8512(2)	−0.10118(3)	0.0143(2)
Fe(4)	4*e*		0.4242(1)	−0.3404(2)	−0.13249(3)	0.0095(2)
X(1)	4*e*	0.68/0.32	0.1377(1)	−0.2168(2)	0.01490(4)	0.0240(3)
X(2)	4*e*	0.45/0.55	0.6000(1)	−0.2714(2)	−0.03640(3)	0.0219(2)
X(3)	4*e*	0.37/0.63	0.1320(1)	−0.8688(2)	−0.23318(3)	0.0221(2)
O(1)	4*e*		0.7621(4)	−0.9943(8)	−0.1104(1)	0.009(1)
O(2)	4*e*		−0.0401(4)	−0.1528(8)	−0.1571(1)	0.009(1)
O(3)	4*e*		0.6099(4)	−0.5063(8)	−0.1261(1)	0.010(1)
O(4)	4*e*		−0.1573(4)	−0.6489(8)	−0.1689(1)	0.010(1)
O(5)	4*e*		0.1053(5)	−0.6349(9)	−0.1395(1)	0.011(1)
O(6)	4*e*		0.3648(5)	−0.5158(9)	−0.1756(1)	0.013(1)
O(7)	4*e*		0.2396(4)	−0.1494(9)	−0.1399(1)	0.011(1)
O(8)	4*e*		0.3081(5)	−0.0346(9)	−0.0593(1)	0.015(1)
O(9)	4*e*		−0.3080(5)	−0.1224(9)	−0.1816(1)	0.012(1)
O(10)	4*e*		0.0305(4)	−0.0149(9)	−0.0864(1)	0.011(1)
O(11)	4*e*		−0.1205(5)	−0.4939(8)	−0.0987(1)	0.009(1)
O(12)	4*e*		0.4866(5)	0.0098(9)	−0.1240(1)	0.014(1)
O(13)	4*e*		0.3676(5)	−0.5392(9)	−0.0907(1)	0.012(1)
O(14)	4*e*		0.6113(5)	−0.6195(9)	−0.2047(1)	0.013(1)
O(15)	4*e*		0.3997(5)	−0.4944(9)	−0.2487(1)	0.016(1)
O(16)	4*e*		0.1308(5)	−0.4993(9)	−0.0625(1)	0.014(1)
(c)						
Te(1)	2*i*		0.8247(2)	0.29932(9)	0.6485(1)	0.0082(3)
Te(2)	2*i*		1.0861(2)	0.07128(9)	0.2001(1)	0.0083(3)
Te(3)	2*i*		0.5974(2)	0.38968(9)	1.2306(1)	0.0092(3)
Fe(1)	1*c*		1	1/2	1	0.0099(6)
Fe(2)	2*i*		0.2961(4)	0.0479(2)	0.5875(2)	0.0104(5)
Fe(3)	2*i*		0.5105(4)	−0.1975(2)	0.0881(2)	0.0121(5)
Cl(1)	2*i*		0.7569(8)	−0.3695(4)	−0.4458(4)	0.0188(8)
O(1)	2*i*		0.699(2)	−0.496(1)	−0.176(1)	0.012(2)
O(2)	2*i*		0.579(2)	−0.217(1)	−0.122(1)	0.016(2)
O(3)	2*i*		0.785(2)	0.065(1)	0.938(1)	0.011(2)
O(4)	2*i*		0.731(2)	0.373(1)	1.049(1)	0.011(2)
O(5)	2*i*		0.366(2)	0.0566(9)	0.383(1)	0.008(2)
O(6)	2*i*		0.452(2)	−0.2138(9)	0.291(1)	0.010(2)
O(7)	2*i*		1.063(2)	−0.1324(9)	0.467(1)	0.008(2)
O(8)	2*i*		0.798(2)	−0.0463(9)	0.217(1)	0.009(2)
O(9)	2*i*		0.103(2)	−0.666(1)	−0.161(1)	0.011(2)

[a] U(eq) is defined as one-third of the trace of the orthogonalized U tensor.

Table 3
Selected bond lengths (Å) for (a) $Cu_3Fe_8Te_{12}O_{32}Cl_{10}$, (b) $Fe_8Te_{12}O_{32}Cl_3Br_3$, and (c) $Fe_5(TeO_3)_6Cl_2$

(a)		Te(4)–O(1)	1.902(4)	Fe(4)–O(6)	1.899(4)
Te(1)–O(3)	1.880(6)	Te(4)–O(12)^{vii}	1.860(5)	Fe(4)–O(7)	2.081(4)
Te(1)–O(3)^{i}	1.880(6)	Te(4)–X(2)	3.106(1)		
Te(1)–O(2)	1.949(8)	Te(4)–O(3)	1.958(4)	*(c)*	
Te(1)–Cl(1)^{ii}	2.950(4)	Te(5)–X(1)	2.920(1)	Te(1)–O(9)^{xii}	1.89(1)
Te(2)–O(1)	1.937(6)	Te(5)–X(2)	2.877(1)	Te(1)–O(6)^{xiv}	1.89(1)
Te(2)–O(4)^{iii}	1.832(6)	Te(5)–O(13)	1.980(5)	Te(1)–O(7)^{xv}	1.940(9)
Te(2)–O(5)	1.936(4)	Te(5)–O(16)	2.047(5)	Te(1)–O(1)^{xvi}	2.491(9)
Te(2)–Cl(3)	3.007(2)	Te(5)–O(8)	1.828(4)	Te(2)–O(3)^{xv}	1.864(9)
Fe(1)–O(1)	2.024(6)	Te(6)–X(3)	3.080(1)	Te(2)–O(5)^{xvii}	1.94(1)
Fe(1)–O(1)^{iv}	2.176(6)	Te(6)–O(14)	1.949(5)	Te(2)–O(3)^{xviii}	2.49(1)
Fe(1)–O(2)^{iv}	1.987(4)	Te(6)–O(15)	1.847(5)	Te(2)–O(2)^{xix}	2.58(1)
Fe(1)–O(3)	2.056(6)	Te(6)–O(15)^{xi}	2.546(5)	Te(2)–O(8)	1.921(9)
Fe(1)–O(3)^{v}	2.010(6)	Te(6)–O(6)	1.911(4)	Te(3)–Cl(1)^{xiv}	2.993(5)
Fe(1)–O(4)	1.927(6)	Fe(1)–O(10)^{vii}	1.963(5)	Te(3)–O(1)^{xiv}	1.88(1)
Cu(1)–Cl(2)	2.038(4)	Fe(1)–O(11)	2.027(4)	Te(3)–O(2)^{xiv}	1.88(1)
Cu(1)–Cl(2)^{vi}	2.038(4)	Fe(1)–O(1)^{viii}	2.054(4)	Te(3)–O(4)	1.92(1)
Cu(2)–Cl(1)^{ii}	2.262(5)	Fe(1)–O(2)^{vii}	2.016(4)	Fe(1)–O(1)^{xv}	1.92(1)
Cu(2)–Cl(2)	2.402(6)	Fe(1)–O(4)	2.027(4)	Fe(1)–O(1)^{xvi}	1.92(1)
Cu(3)–Cl(1)	2.349(5)	Fe(1)–O(5)	1.958(5)	Fe(1)–O(4)	2.06(1)
Cu(3)–Cl(2)	2.449(5)	Fe(2)–O(11)	2.135(4)	Fe(1)–O(4)^{xx}	2.06(1)
		Fe(2)–O(1)^{xii}	2.084(4)	Fe(1)–O(9)^{xiii}	2.103(9)
(b)		Fe(2)–O(2)	2.101(4)	Fe(1)–O(9)^{xiv}	2.103(9)
Te(1)–O(2)	1.936(5)	Fe(2)–O(3)^{viii}	1.980(4)	Fe(2)–O(5)	2.030(1)
Te(1)–O(5)	1.896(4)	Fe(2)–O(4)	1.980(4)	Fe(2)–O(5)^{xiv}	1.98(1)
Te(1)–O(6)	2.575(5)	Fe(2)–O(9)	1.888(5)	Fe(2)–O(6)^{xiv}	2.00(1)
Te(1)–O(7)	1.889(4)	Fe(3)–O(10)^{vii}	2.099(5)	Fe(2)–O(7)^{xiv}	1.99(1)
Te(2)–O(14)^{viii}	1.918(5)	Fe(3)–O(13)	2.195(5)	Fe(2)–O(7)^{xxi}	2.065(9)
Te(2)–O(15)^{ix}	2.305(5)	Fe(3)–O(16)	2.427(5)	Fe(2)–O(8)^{xiv}	1.98(1)
Te(2)–O(4)	1.986(4)	Fe(3)–O(5)	2.084(5)	Fe(3)–O(2)	2.01(1)
Te(2)–O(9)^{vii}	1.855(4)	Fe(3)–O(7)^{vii}	2.079(4)	Fe(3)–O(3)^{xiv}	2.024(1)
Te(3)–X(1)^{x}	3.063(1)	Fe(3)–O(8)^{vii}	2.002(5)	Fe(3)–O(4)^{xiv}	2.08(1)
Te(3)–O(10)	1.900(4)	Fe(4)–O(12)	1.886(5)	Fe(3)–O(6)	2.01(1)
Te(3)–O(11)	1.916(4)	Fe(4)–O(13)	1.921(5)	Fe(3)–O(8)	2.00(1)
Te(3)–O(16)	1.925(5)	Fe(4)–O(3)	2.032(4)	Fe(3)–O(9)^{xxii}	2.45(1)

Symmetry codes: (i) x, $0.5-y$, z; (ii) x, y, $-1+z$; (iii) x, y, $1+z$; (iv) $2-x$, $-y$, $1-z$; (v) $2-x$, $-y$, $-z$; (vi) $1.5-x$, $0.5-y$, z; (vii) x, $-1+y$, z; (viii) $-1+x$, y, z; (ix) $-x$, $-0.5+y$, $-0.5-z$; (x) $-x$, $-1-y$, $-z$; (xi) $1-x$, $-0.5+y$, $-0.5-z$; (xii) $-1+x$, $1+y$, z; (xiii) $1+x$, $1+y$, $1+z$; (xiv) $1-x$, $-y$, $1-z$; (xv) $2-x$, $-y$, $1-z$; (xvi) x, $1+y$, $1+z$; (xvii) $1+x$, y, z; (xviii) x, y, $-1+z$; (xix) $2-x$, $-y$, $-z$; (xx) $2-x$, $1-y$, $2-z$; (xxi) $-1+x$, y, z; (xxii) $1-x$, $-1-y$, $-z$.

3.2. The crystal structure of $Fe_8Te_{12}O_{32}Cl_3Br_3$ (II)

II crystallizes in the monoclinic system, space group $P2_1/c$. The structure is layered perpendicular to [001] with two types of non-bonding regions, see Fig. 4a.

Table 4
Calculated BVS values for the ions in I–III according to Brown [29]

(I) $Cu_3Fe_8Te_{12}O_{32}Cl_{10}$					
Te(1)	3.89	Cu(3)	0.94	O(2)	2.18
Te(2)	3.89	Cl(1)	0.81	O(3)	2.27
Fe(1)	2.89	Cl(2)	1.05	O(4)	2.03
Cu(1)	1.23	Cl(3)	0.83	O(5)	2.23
Cu(2)	1.13	O(1)	1.94		
(II) $Fe_8Te_{12}O_{32}Cl_3Br_3$					
Te(1)	3.83	X(1)	0.46	O(8)	1.94
Te(2)	3.95	X(2)	0.53	O(9)	2.11
Te(3)	3.75	X(3)	0.20	O(10)	2.16
Te(4)	3.83	O(1)	2.10	O(11)	2.04
Te(5)	3.93	O(2)	2.03	O(12)	2.09
Te(6)	4.11	O(3)	2.10	O(13)	1.91
Fe(1)	3.13	O(4)	2.03	O(14)	2.25
Fe(2)	3.03	O(5)	2.19	O(15)	2.05
Fe(3)	1.90	O(6)	2.11	O(16)	2.12
Fe(4)	3.01	O(7)	2.05		
(III) $Fe_5(TeO_3)_6Cl_2$					
Te(1)	3.92	Fe(3)[2]	2.21	O(4)	1.99
Te(2)	4.07	Fe(3)[3]	2.37	O(5)	2.14
Te(3)	3.94	Cl(1)	0.18	O(6)	2.25
Fe(1)	3.01	O(1)	2.21	O(7)	2.10
Fe(2)	3.12	O(2)	1.95	O(8)	2.20
Fe(3)[1]	2.63	O(3)	2.07	O(9)	2.10

The r_0 values used were: $r_0 = 1.977$ for Te^{4+}–O bonds [28], $r_0 = 2.37$ for Te^{4+}–Cl bonds [30], $r_0 = 2.55$ for Te^{4+}–Br bonds [31], $r_0 = 1.70$ for Fe^{2+}–O bonds [31], $r_0 = 1.765$ for Fe^{3+}–O bonds [32] and $r_0 = 1.858$ for Cu^{+}–Cl bonds [33].
[1–3]The three BVS values for Fe(3) in **III** has been calculated with: (1) Fe as a Fe^{3+} ion, (2) Fe as a Fe^{2+} ion and (3) Fe as a mixture of Fe^{2+} and Fe^{3+}.

The compound has only been found with a mixture of Cl and Br on the halide sites, so refinement of the individual occupancies for Cl and Br has been performed. These gave 68% Cl and 32% Br for *X*(1), 45% Cl and 55% Br for *X*(2), and 37% Cl and 63% Br for *X*(3), yielding an average of 50% for each of the halides, which result in the formula $Fe_8Te_{12}O_{32}Cl_3Br_3$. EDS analysis on the crystal used for single crystal X-ray diffraction data determined the amounts of the heavy atoms to be 29.0 ± 0.4 at% Fe, 46.2 ± 0.7 at% Fe, 12.7 ± 0.8 at% Cl and 12.1 ± 0.8 at% Br, which is in good agreement with the results from the refinement of single crystal diffraction data (the errors have been estimated from ten different analysis on the same crystal). BVS calculations and the resulting limit for the primary coordination sphere for the Te–*X* bonds have been performed taking into account the mixed occupancy of Cl and Br at the halide sites.

There are six crystallographically different Te^{4+} that all show an asymmetric coordination due to the stereochemically active lone–pair electrons. Te(1) and Te(2) both coordinate to four oxygen atoms with three shorter distances, 1.855(4)–1.986(4) Å, and one longer, 2.305(5)–2.575(5) Å, resulting in $[TeO_{3+1}E]$ trigonal bipyramides. Te(3) and Te(4) both coordinate to three oxygen atoms with Te–O distances in the range 1.900(4)–1.958(4) Å, and one halide atom at the distance 3.064(1) and 3.106(1) Å,

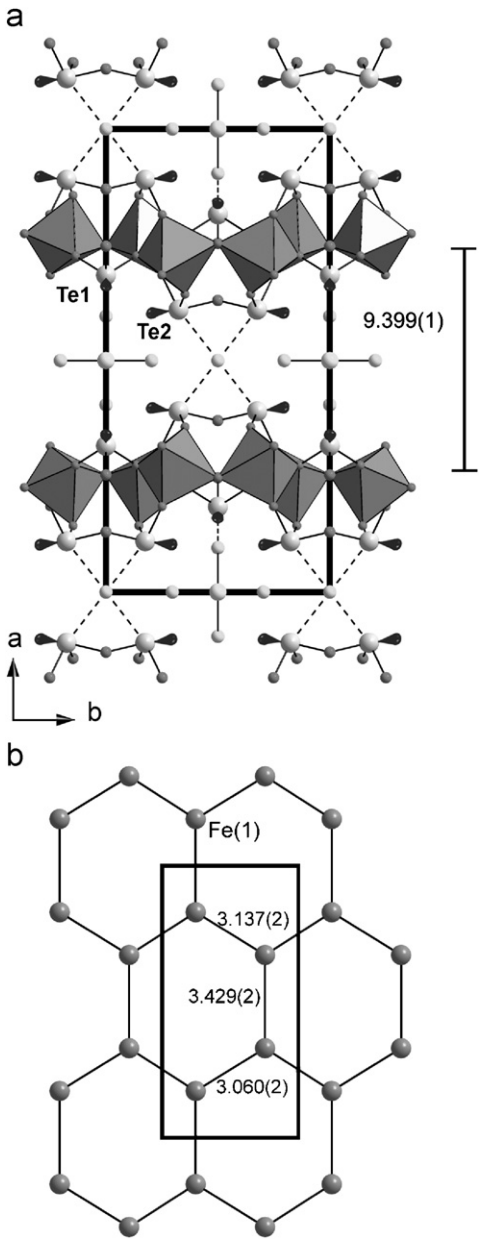

Fig. 1. (a) The structure of $Cu_3Fe_8Te_{12}O_{32}Cl_{10}$ seen along the [001]. The iron ions are shown in oxygen polyhedra while the tellurium and copper ions are shown with ligands. The lone–pair is shown with an orbital shape. Te–Cl bonds are dashed. The shortest Fe–Fe distance in between two layers is given. (b) The honeycomb lattice arrangement of the Fe layers.

respectively. Those latter distances are at the boundary of the primary coordination sphere, and the coordination can be regarded as being a distorted $[TeO_3XE]$ trigonal bipyramid. Te(5) have three short Te–O distances, 1.828(4)–2.047(5) Å and two comparatively short Te–*X* distances at 2.877(1) and 2.920(1) Å resulting in a highly distorted $[TeO_3X_2E]$ octahedron. Finally Te(6) coordinate four oxygens and one halide; three of the Te–O distances are shorter, 1.847(5)–1.949(5) Å, and the fourth is longer, 2.546(5) Å. The Te–*X* distance is 3.080(1) Å, again a distance that can be considered to be at the

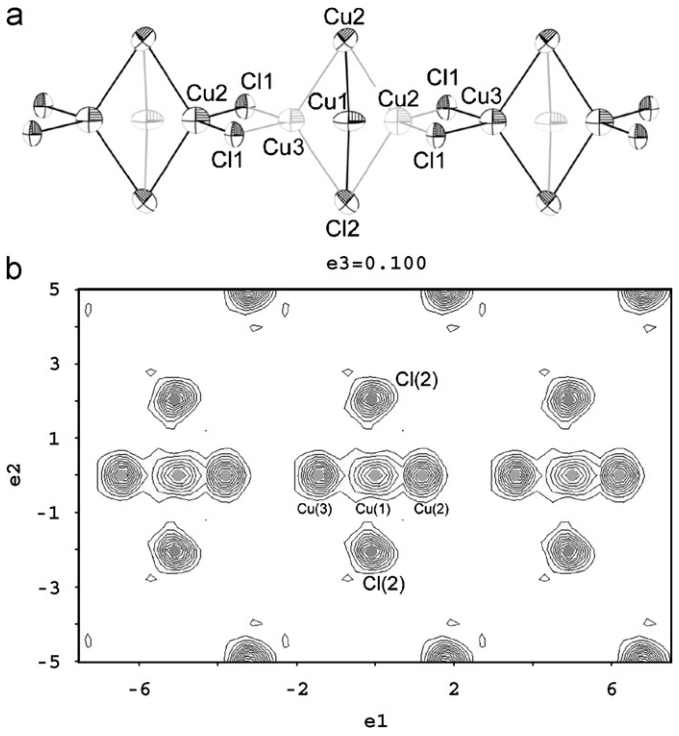

Fig. 2. (a) The thermal ellipsoids of the central part of the Cu–Cl chain in $Cu_3Fe_8Te_{12}O_{32}Cl_{10}$. The Cu chains extend along [001] and are made up of two edge sharing Cu tetrahedra with a Cu^+ on one of the shared edges. The Cu^+ are half-occupied sites, which means that only every second site is occupied at the same time. The partly transparent atoms indicate sites that then should be unoccupied. (b) The electron density map with a positive cut off at $2\,e^-/Å^3$ of the three Cu sites.

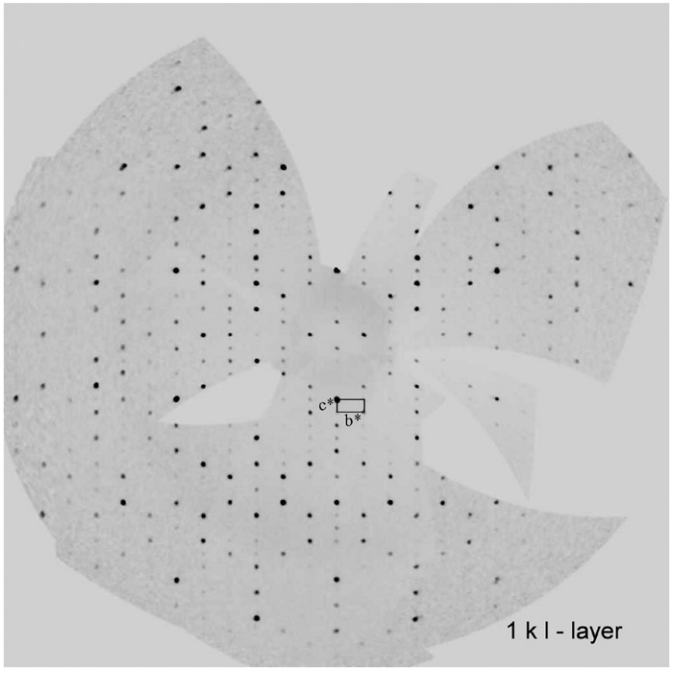

Fig. 3. The $1\,k\,l$ diffraction pattern of $Cu_3Fe_8Te_{12}O_{32}Cl_{10}$. No evidence of a doubling of the c-axis can be seen.

verge of the primary coordination sphere; the resulting polyhedron is a highly distorted $[TeO_{3+1}XE]$ octahedron.

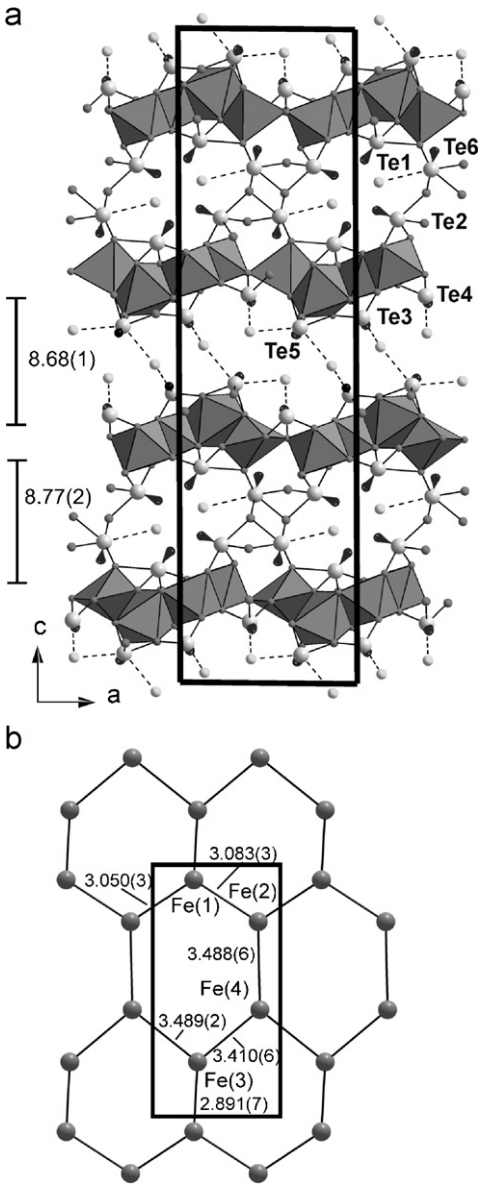

Fig. 4. (a) The structure of $Fe_8Te_{12}O_{32}Cl_3Br_3$ seen along [010]. The labelling is the same as for Fig. 1a. The Te–Cl bonds are dashed. The shortest Fe–Fe distances in between the layers are given. (b) The honeycomb lattice arrangement of the Fe atoms.

There are four crystallographically different Fe atoms in the compound. Three of these, Fe(1), Fe(2), and Fe(3), show octahedral coordinations to six oxygen, while Fe(4) has a trigonal bipyramidal coordination to five oxygen. Layers are built by corner and edge sharing of $[FeO_6]$ and $[FeO_5]$ polyhedra, see Fig. 4a. The Fe atoms are arranged into a honeycomb lattice, see Fig. 4b.

The Te-polyhedra connect two layers of Fe-polyhedra so that two types of non-bonding regions are formed by the stereochemically active lone–pairs on Te^{4+}; layers perpendicular to [001] and channels along [010]. The weak Te–X bonds connects the Fe–Te–O layers, see Fig. 4a. $X(3)$ that is positioned within the channels receives a BVS value of 0.20 vu if only the primary Te–X interactions are included,

while $X(1)$ and $X(2)$ get BVS values of ~0.5 vu, see Table 4. None of the halides can thus be considered as being fully integrated in the ionic/covalent network, and instead they partly take the role as counter ions.

Charge neutrality can only be achieved if the compound comprises a mixture of Fe^{3+} and Fe^{2+}. The eight iron ions in the chemical formula should balance a net charge of −22 from the anions and Te^{4+}. This means an average charge for the Fe ions of +2.75, or a three to one favour of Fe^{3+} over Fe^{2+}. BVS calculations were used to check the valence of each of the Fe sites and yields that Fe(3) gets a value rather close to +2 while Fe(1), Fe(2), and Fe(4) get values close to +3, see Table 4.

3.3. The crystal structure of $Fe_5(TeO_3)_6Cl_2$ (III)

III crystallizes in the triclinic system, space group $P\bar{1}$. EDS-data based on analyses of eight different crystals determines the amount of the heavy atoms to be 36.9±0.7 at% Fe, 46.1±0.6 at% Te and 17.0±0.7 at% Cl, and this is in reasonable agreement with the results from the refinement of single crystal data. The structure is layered with channels along [100], see Fig. 5a. The structure was solved from a twin were the second component was rotated along [010].

There are three crystallographically different Te^{4+} that all have one-sided asymmetric coordinations due to the presence of the stereochemically active lone–pair electrons. Te(1) has a $[TeO_{3+1}E]$ coordination with three shorter, 1.89(1)–1.94(1) Å, and one longer, 2.49(1) Å, bond distance. Te(2) has a highly distorted coordination to five oxygen; three shorter, 1.86(1)–1.94(1) Å, and two longer, 2.49(1)–2.58(1) Å, bonds resulting in a $[TeO_{3+2}E]$ octahedron. Te(3) coordinate three oxygen and it has a Cl at 2.99(1) Å away, which is at the verge of being considered as primary coordinated, to fulfil a $[TeO_3ClE]$ trigonal bipyramid. However, BVS calculations gives very low valences for these Cl ions, ~0.19 vu if only the primary bonds are taken into account, indicating that they mainly take a role as counter ions.

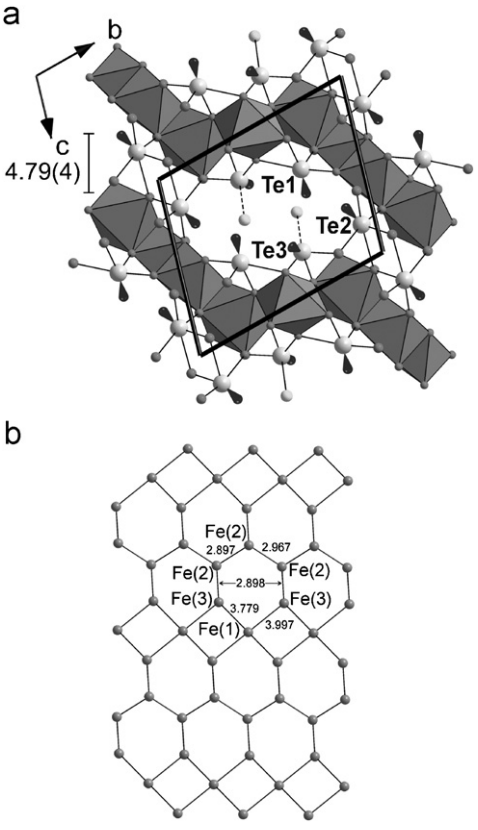

Fig. 5. (a) The structure of $Fe_5(TeO_3)_6Cl_2$ seen along [100]. The labelling is the same as for Fig. 1a. The Te–Cl bonds are dashed. The shortest Fe–Fe distance in between two layers is given. (b) The honeycomb variant lattice arrangement of the Fe atoms.

There are three crystallographically different Fe atoms that all have distorted $[FeO_6]$ octahedral coordinations, with Fe–O distances in the range 1.92(1)–2.45(1) Å. These Fe atoms are arranged into a honeycomb variant lattice arrangement with edge sharing hexagons and squares, see Fig. 5b.

The $Fe_5(TeO_3)_6Cl_2$ structure can be considered as layered, where the $[FeO_6]$ octahedra are connected by edge and corner sharing. The various polyhedra around the Te^{4+} ions connect to the Fe–O layers via edge and corner sharing through common oxygen ions. $[Te(2)O_{3+2}E]$ units connect the layers via their long Te–O bonds so that channels are formed running along [100]. The lone–pairs on Te^{4+} are pointing inwards into those channels, were also the two Cl atoms are residing, see Fig. 5a. Each of the Cl atoms is coordinated to only one Te via a long primary bond, but both of the Cl atoms have five additional Te atoms just outside the primary coordination sphere at distances around 3.2–3.3 Å forming distorted $[ClTe_6]$ octahedra. If these five interactions are included in the BVS calculations the valence for Cl goes up to ~0.62 vu, a large increase from the initial ~0.19 vu, but still far from the expected value of one.

For charge neutrality to be reached in the formula $Fe_5(TeO_3)_6Cl_2$, the total charge of the Fe-ions must be +14. This means an average of +2.8 vu for each Fe atom, and a mixture of Fe^{3+} and Fe^{2+} is needed. BVS calculations do not reveal any specific Fe position with a value low enough to be considered as being occupied solely by Fe^{2+}. However, Fe(3) has a BVS value lower than three indicating that this site is occupied by a mixture of Fe^{2+} and Fe^{3+}, see Table 4. BVS calculations allowing for a valence mixing according to Brown [13], propose that Fe(3) is occupied by 36% Fe^{3+} and if this percentage is used for calculating the average BVS value of the Fe(3) site, then the valence sum for all the Fe-ions will be +13.98 vu in **III**, a value which is close to the expected +14.

4. Discussion

4.1. The Te^{4+} coordinations

The halide ions in **I**–**III** are all positioned at distances so close to Te^{4+} that they can be considered as being inside

the limit of the primary coordination sphere of the lone–pair cation. However, the Te–Cl/Br bonds are weaker than the Te–O bonds. Weak Te–X bonds that are on the verge of being considered to belong to the primary bonding sphere has been observed in other transition metal tellurite halide compounds before [4,5], but not with the halide ion clearly inside the primary coordination sphere.

Te^{4+} has almost only been observed accepting oxygen ligands in transition metal tellurite halides; the coordination is then $[TeO_3E]$ or $[TeO_{3+1}E]$. $FeTe_2O_5X$ (X = Cl, Br) is the only compound with a $[TeO_2XE]$ coordination [8], due to the high strength of the Fe–O bonds that forced Te^{4+} to accept also halides as ligands. In the new compounds presented in this work the results point in a similar direction; the Fe–O bonds are stronger than the Te–O bonds forcing Te^{4+} to accept also halides as ligands. Table 5 shows a summary of the Te-coordinations for compounds **I**–**III**.

It is striking to note that not a single one of all the crystallographically different Te^{4+} in these compounds takes the common tetrahedral $[TeO_3E]$ coordination but instead takes larger coordinations. Also observations of octahedrally coordinated Te^{4+} (five ligands plus the stereochemically active lone–pair) are scarce, but the existence of a fifth ligand around Te^{4+} has been discussed before. However, no previously described compound has a fifth ligand inside the primary coordination sphere [20,21].

4.2. The Fe layers

The Fe atoms are arranged into distorted honeycomb lattices in both **I** and **II**, see Figs. 1b and 4b. **III** has the Fe atoms arranged into a variant of the honeycomb lattice with edge sharing hexagons interrupted by rows of squares, see Fig. 5b. The intra-layer Fe–Fe distances are in the range 2.9–4.0 Å for all three compounds. The honeycomb lattices in **I** and **II** are puckered and slightly distorted, and the Fe–Fe distances within the hexagons vary by a few tenths of an Å. The ideal hexagonal angle is 120° but due to the puckering of the layers of **I** and **II**, the angles vary as much as in between 93° and 128°. For **III** the honeycomb lattice is interrupted by rows of square planes that have common edges with the hexagons. The squares actually take the form of a parallelogram with Fe–Fe distances at 3.78(16) and 4.00(14) Å.

Table 5
Summary of the local coordination for all the crystallographic different Te^{4+} in **I–III**

(I) $Cu_3Fe_8Te_{12}O_{36}Cl_{10}$	(II) $Fe_8Te_{12}O_{36}Cl_3Br_3$	(III) $Fe_5(TeO_3)_6Cl_2$
$[Te(1)O_3ClE]$	$[Te(1)O_{3+1}E]$	$[Te(1)O_{3+1}E]$
$[Te(2)O_3ClE]$	$[Te(2)O_{3+1}E]$	$[Te(2)O_{3+2}E]$
—	$[Te(3)O_3XE]$	$[Te(3)O_3ClE]$
—	$[Te(4)O_3XE]$	—
—	$[Te(5)O_3X_2E]$	—
—	$[Te(6)O_{3+1}XE]$	—

Among oxohalides, the compound $Sr_2Cu_2TeO_6Br_2$ show a distorted honeycomb lattice of Cu^{2+} ions [22]. Honeycomb lattice arrangements of Fe atoms are relatively uncommon, however, some few compounds with such an arrangement have previously been reported, e.g. $FePSe_3$ and $FePS_3$, both with Fe^{3+} [23,24]. Some hexagonal perovskites also show tendencies towards honeycomb like lattices of Fe^{3+} [25], and a few organometallic compounds with such an arrangement of Fe^{2+} as well as with Fe^{3+} are also known [26–28].

4.3. The non-bonding regions

The existence of non-bonding regions that are occupied by the stereochemically active lone–pairs as well as the halides is a common and expected feature for oxohalide compounds of this type. Such features can in principle take three different forms; layered, tubular, or spherical, were the former two are the most common types, and both these types are present in the new compounds described in this work; **I** has tubular channels along [001], see Fig. 1a, **II** has layered regions parallel to the *ab*-plane as well as tubular channels along [010], see Fig. 4a, and **III** has tubular channels along [100], see Fig. 5a. There is thus space in the non-bonding regions in all the compounds to accommodate the stereochemically active lone–pairs as well as the counter ions.

The ions always constitute halides that are weakly bonded to the surrounding Te^{4+} with a BVS value much lower than the expected one, so the halides can thus not be regarded as being fully bonded to the ionic/covalent network. For **I** there also exist Cu–Cl chains within one such tubular channel, which means that the tubular channel does not constitute a non-bonding regions *per se*, but the lone–pairs still point towards the halides as would be the case if the Cu–Cl chains were not present so they can also be regarded as channels of the non-bonding type.

4.4. The chemical role of the halides

The halides in **II** and **III** have a choice to bond to Fe^{3+}/Fe^{2+} or Te^{4+}, however, none of those cations are eager to bond to such a weak Lewis base when oxygen is available. The halides in **I** have the option to bond to Cu^{+} instead, a rather weak Lewis acid, which also is what occurs. Halides in a surrounding with strong and/or moderately strong Lewis acids will only bond weakly to these, and will typically receive a BVS value considerably lower than the expected value of one. Halides in a surrounding with weak Lewis acids will instead form rather strong bonds to these with resulting BVS values close to the expected one. Halides in a strong Lewis acid surrounding will hence more act as counter ions, while halides in a weak Lewis acid surrounding will instead take a more active role in the covalent/ionic network.

5. Conclusions

Three new compounds; $Cu_3Fe_8Te_{12}O_{32}Cl_{10}$, $Fe_8Te_{12}O_{32}Cl_3Br_3$, and $Fe_5(TeO_3)_6Cl_2$, have been synthesized via chemical reactions in sealed and evacuated silica tubes, and their crystal structures are described. The synthesis temperatures were 500–540 °C. All three compounds have layered structures with weak secondary Te–O or Te–Cl/Br bonds holding the layers together. Each layer constitutes iron–oxygen polyhedra where the iron atoms are arranged into variants of the honeycomb lattice.

The commonly observed [TeO_3E] tetrahedron coordination is abandoned by Te^{4+} for all the Te atoms in favour of larger coordination polyhedra that include halides due to the formation of comparatively strong Fe–O bonds. These stronger bonds forces Te^{4+} to accept halides as ligands, although their high Lewis acid strength regularly allows them to bond only to oxygen in an oxo-halide.

The halides in $Fe_8Te_{12}O_{32}Cl_3Br_3$ and $Fe_5(TeO_3)_6Cl_2$ are only weakly bonded to Te^{4+} and thereby take the role of counter ions with a resulting low bond valence sum value. The halides in the Cu-containing compound is also weakly bonded to Te^{4+}, but are additionally strongly bonded to Cu and are hence fully integrated into the covalent/ionic network. The halides are, together with the stereochemically active lone–pair electrons on Te^{4+}, positioned in volumes of non-bonding regions, which give the structures their low-dimensional character.

Acknowledgments

Prof. Sven Lidin for valuable discussions. This work has been carried out through financial support from the Swedish Research Council.

Appendix A. Supplementary materials

Supplementary data associated with this article can be found in the online version at doi:10.1016/j.jssc.2007.03.013.

References

[1] M. Johnsson, K.W. Törnroos, F. Mila, P. Millet, Chem. Mater. 12 (2000) 2853–2857.
[2] M. Johnsson, K.W. Törnroos, P. Lemmens, P. Millet, Chem. Mater. 15 (2003) 68–73.
[3] R. Becker, M. Johnsson, R.K. Kremer, P. Lemmens, Solid State Sci. 5 (11–12) (2003) 1411–1416.
[4] R. Becker, M. Johnsson, R.K. Kremer, P. Lemmens, J Solid State Chem. 178 (2005) 2024–2029.
[5] R. Becker, H. Berger, M. Johnsson, M. Prester, Z. Marohnic, M. Miljak, M. Herak, J Solid State Chem. 179 (2006) 836–842.
[6] R. Takagi, M. Johnsson, V. Gnezdilov, R.K. Kremer, W. Brenig, P. Lemmens, Phys. Rev. B 74 (2006) 014413.
[7] Z. Mayerová, M. Johnsson, S. Lidin, Angew. Chem. Int. Ed. 45 (2006) 5602–5606.
[8] R. Becker, M. Johnsson, R.K. Kremer, H.-H. Klauss, P. Lemmens, J. Am. Chem. Soc. 128 (2006) 15469–15475.
[9] Oxford Diffraction Ltd., Xcalibur CCD System, CysAlis Software System CCD, version 1.171.29.2, Poland, 2006.
[10] Oxford Diffraction Ltd., Xcalibur CCD System, CysAlis Software System RED, version p.171.29.2, Poland, 2006.
[11] G.-M. Sheldrick, SHELXS-97—Program for the Solution of Crystal Structures, Göttingen, 1997.
[12] G.-M. Sheldrick, SHELXL-97—Program for the Refinement of Crystal Structures, Göttingen, 1997
[13] I.D. Brown, The Chemical Bond in Inorganic Chemistry: The Bond Valence Model, Oxford University Press, New York, 2002.
[14] B.U. Koehler, M. Jansen, Z. Anorg. Allg. Chem. 543 (1986) 73–80.
[15] M. Louer, R. Brochu, D. Louer, S. Arsalane, M. Ziyad, Acta Crystallogr. B 51 (1995) 908–913.
[16] C. Burschka, Z. Anorg. Allg. Chem. 463 (1980) 65–71.
[17] M.E. Fleet, Acta Crystallogr. B 37 (1981) 917–920.
[18] I.E. Grey, D.J. Lloyd, Acta Crystallogr. B 32 (1976) 1509–1513.
[19] J.S. Swinnea, H. Steinfink, Am. Mineralog. 68 (1983) 827–832.
[20] J. Zemann, Monatsh. Chem. 102 (5) (1971) 1209–1216.
[21] F. Pertlik, J. Zemann, Anzeiger Oesterreichischen Akad. Wissensch. Mathematisch-Naturwissensch Klasse 3 (13) (1971) 175–176.
[22] R. Takagi, M. Johnsson, Acta Crystallogr. C 62 (2006) i38–i40.
[23] A. Wiedenmann, J. Rossat-Mignod, A. Louisy, R. Brec, J. Rouxel, Solid State Commun. 40 (1981) 1067–1072.
[24] G. Ouvrard, R. Brec, J. Rouxel, Mater. Res. Bull. 20 (1985) 1181–1189.
[25] N.A. Jordan, P.D. Battle, J. Sloan, P. Manuel, S. Kilcoyne, J. Mater. Chem. 13 (10) (2003) 2617–2625.
[26] C.S. Hong, Y.S. You, Inorg. Chim. Acta 357 (11) (2004) 3271–3278.
[27] Y.-C. Jiang, S.-L. Wang, S.-F. Lee, K.-H. Lii, Inorg. Chem. 42 (20) (2003) 6154–6156.
[28] E. Colacio, J.M. Dominguez-Vera, M. Ghazi, J.M. Moreno, R. Kivekas, F. Lloret, H. Stoeckli-Evans, Chem. Commun. (Cambridge) 11 (1999) 987–988.
[29] I.D. Brown, D. Altermatt, Acta Crystallogr. B 41 (1985) 244–247.
[30] N.E. Brese, M. O'Keeffe, Acta Crystallogr. B 47 (1991) 192–197.
[31] C. Hormillosa, S. Healy, T. Stephen, 1993. Program Bond Valence Calculator 2.00.
[32] W. Liu, H.H. Thorp, Inorg. Chem. 32 (1993) 4102–4105.
[33] G.P. Shields, P.R. Raithby, F.H. Allen, W.D.S. Motherwell, Acta Crystallogr. B 56 (1999) 455–465.